Solution of the growth equations of a sector of a polymer crystal including consideration of the changing size of the crystal

Marc L. Mansfield
Michigan Molecular Institute, 1910 West St Andrews Road, Midland, Michigan 48640, USA
(*Received 1 February 1988; revised 12 April 1988; accepted 20 April 1988*)

We obtain a solution for the nucleation-controlled growth of a sector of a polymer single crystal that treats directly the changing size of the crystal. The problem is treated by solving a pair of differential equations with moving boundary conditions. A steady-state solution is obtained for the case in which the two boundaries move apart at the same rate. The steady-state solution is inherently regime II for all possible values of the model parameters. The growth-front profile is a section of an ellipse.

(Keywords: growth equations; crystal; moving boundary conditions)

INTRODUCTION

The standard nucleation model of polymer crystal growth[1] assumes that crystallization occurs by a sequence of steps summarized in *Figure 1*. Addition of a new layer to an existing crystal substrate requires a nucleation step, in which a single stem lays down on the substrate, as depicted in *Figure 1a*. We let i denote the nucleation rate per unit length along the substrate (dimensions = length^{-1} time^{-1}). After this nucleation step, subsequent stems lay down adjacent to the first in what is usually called the substrate completion process, as shown in *Figure 1b*. Each edge of the new patch grows with a rate g (dimensions = length time^{-1}). We let b represent the thickness of the patch.

The advance of patches on the substrate is arrested in one of three ways, as shown in *Figure 2*. Interpretation of crystal growth-rate data indicates that substrate completion does not extend beyond a representative length, the substrate length, denoted here as L. This is illustrated in *Figure 2a*. The reason for this behaviour is not understood, although either crystal defects[2] or regions of imperfect lattice coherence (both occurring with mean separation L) may be responsible. Another process that arrests patch growth is the collision of a left-moving and a right-moving boundary, as in *Figure 2b*. The third process results from the fact that patches must stop when they reach the end of the crystal, as depicted in *Figure 2c*.

Crystallization is known to occur in three separate regimes, called regimes I, II and III in order of decreasing temperature[1,3]. Regime I occurs when the process depicted in *Figure 2a* dominates. Since i is the nucleation rate per unit length, then iL is the rate at which nucleation occurs at any point within the interval L. Since patches are stopped only at the boundary, each nucleation event gives rise to a complete layer, so that iL is also the rate at which layers form. Therefore, the net growth rate G is given by $G = ibL$ in regime I. Regime II occurs when the process in *Figure 2b* dominates. Then, a number of nucleation events are involved in the creation of a single layer. Therefore, we expect G to be independent of L, but dependent on g. Indeed G proves to be given as $G = b(2ig)^{1/2}$ in regime II. Regime III occurs when nucleation is so rapid that each stem is laid down in a separate nucleation event so that substrate completion is not important. We then expect G to be independent of g once

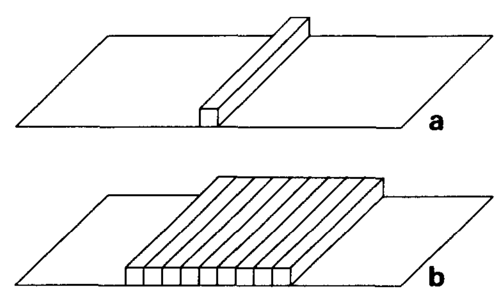

Figure 1 Polymer crystal growth occurs first by a nucleation step, with new stems appearing at a rate i per unit length on the substrate (a). The new patch grows laterally, each side advancing at a rate g in the substrate completion process (b)

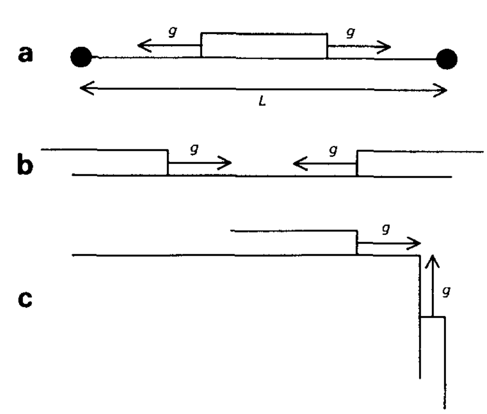

Figure 2 Growing patches on a substrate are arrested in one of three ways: (a) growth is unable to continue beyond distances of the order of L, indicated here by the two full circles separated by a distance L; a collision of left- and right-moving patches stops both patches; (c) growth cannot extend beyond the end of the crystal

0032-3861/88/101755-06$03.00

again. In fact, G is given by $G=\sigma ibL$ in regime III, for σ some factor less than unity.

The process shown in *Figure 2c* does not influence growth rates, but it does influence the morphology of sectored crystals. A crystal will grow with a shape that guarantees that layers growing towards the sector boundary arrive simultaneously from the two sectors, as depicted in *Figure 2c*. This paper provides one example of this effect.

The following equations, proposed by Frank[4], account for crystal growth by this model:

$$\frac{\partial r}{\partial t}+g\frac{\partial r}{\partial x}=-2grl+i \tag{1a}$$

$$\frac{\partial l}{\partial t}-g\frac{\partial l}{\partial x}=-2grl+i \tag{1b}$$

The functions $r(x,t)$ and $l(x,t)$ are the concentrations of right- and left-moving steps on the growth front, each having dimensions of length^{-1}. The quantities g and i are as defined above. Each nucleation event is assumed to produce a pair of steps, one travelling to the right and one to the left, at velocities $\pm g$, respectively. Each step continues to move until it either collides with a step moving in the opposite direction or reaches the boundary. Eigenfunctions of the differential operator

$$\frac{\partial}{\partial t}\pm g\frac{\partial}{\partial x}$$

are functions translating uniformly with velocity $\pm g$. Therefore, the left-hand sides of equations (1) represent the uniform translation of steps. The terms $-2grl$ in equations (1) represent removal of steps through collisions. The terms i represent creation of new steps through nucleation.

Frank[4] and Toda *et al.*[5] have considered solutions to the above set of differential equations. To model the effect shown in *Figure 2a*, they introduced boundary conditions at $x=\pm L/2$ that effectively stop all steps reaching the boundary. In this paper, we consider another possibility, namely that the substrate completion process continues across the entire face of a growing sector. Therefore, we solve equations (1) in a moving interval $-ht<x<ht$, for $2h$ the relative velocity of the two boundaries of the growing sector. The velocity h is determined by the growth of adjoining sectors, and will be taken as a given quantity in this calculation. A more general problem, which we do not consider here, would be to assume that the left and right boundaries move at different rates. This would apply to the growth of a sector bounded by non-equivalent sectors.

We are assuming that the process shown in *Figure 2a* does not occur, and that only the mechanisms shown in *Figures 2b* and *2c* are responsible for halting the growth of individual patches. Our solution, therefore, is inherently regime II. There is also no opportunity of seeing regime III behaviour in any solutions of the above differential equations. The differential equations evolve from a continuity assumption, while regime III is a direct result of the discreteness of the structure at the molecular level.

The complete statement of our problem is as follows: We seek steady-state solutions $r(x,t)$ and $l(x,t)$ obeying:

$$\frac{\partial r}{\partial t}+g\frac{\partial r}{\partial x}=-2grl+i \qquad \text{if } |x|<ht \tag{2a}$$

$$\frac{\partial l}{\partial t}-g\frac{\partial l}{\partial x}=-2grl+i \qquad \text{if } |x|<ht \tag{2b}$$

$$\frac{\partial r}{\partial t}+g\frac{\partial r}{\partial x}=0 \qquad \text{if } |x|>ht \tag{3a}$$

$$\frac{\partial l}{\partial t}-g\frac{\partial l}{\partial x}=0 \qquad \text{if } |x|>ht \tag{3b}$$

subject to the boundary conditions:

$$r(-ht,t)=0 \tag{4a}$$

$$l(ht,t)=0 \tag{4b}$$

The boundary conditions in equations (4) result because no steps enter from outside the limits $x=\pm ht$. Indeed, $r(x,t)=0$ for all $x<-ht$, and $l(x,t)=0$ for all $x>ht$. We also assume that $h<g$. We show below that the case $h>g$ need not be considered.

Equations (3) demand some explanation. We should, of course, remove all right-moving steps reaching the boundary at $x=+ht$ and all left-moving steps reaching $x=-ht$. By writing equation (3), we assume that the steps reaching the boundary continue on past. This artifice is employed to obtain a count of the number of steps that meet the boundary per unit time. Steps outside the boundaries are not considered to be real. The additional boundary condition that r and l are continuous at the boundaries completely determines the problem.

Symmetry requires:

$$r(x,t)=l(-x,t) \tag{5}$$

In the next section we derive the steady-state solution to the above problem. Then we apply the results to predict the shape of a hypothetical, polyethylene-like crystal. In the final section we present some brief discussion.

SOLUTION OF THE DIFFERENTIAL EQUATIONS

We began studying this problem by computer simulation. The simulations provided enough insight to obtain the steady-state solution, and so are not reported here.

We expect:

$$r(ht,t)=l(-ht,t)=N_0 \tag{6}$$

at steady state, for N_0 a constant. Equation (6) is supported by the computer simulations mentioned above. We begin by considering solutions valid outside the boundaries. As stated above, solutions to equation (3a) are any functions translating to the right with velocity g; combining this fact with equation (6) implies the following steady-state behaviour:

$$r(x,t)=\begin{cases} N_0 & \text{for } ht<x<gt+\alpha \\ f_T(x-gt-\alpha) & \text{for } gt+\alpha<x \end{cases} \tag{7}$$

for α some induction distance over which steady-state conditions develop, and f_T some undetermined function representing the steps having escaped before achievement of the steady state. The total number of steps to have 'escaped' from the right side of the system in time interval $(0,t)$ is:

$$\int_{ht}^{\infty} r\,dx=N_0t(g-h)+P \tag{8}$$

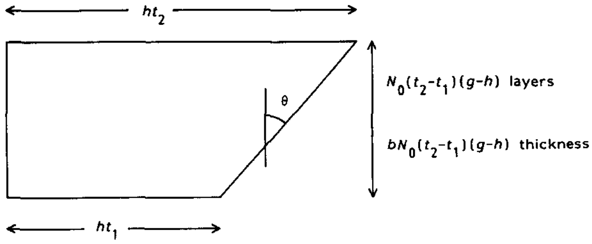

Figure 3 Between $t=t_1$ and $t=t_2$ a total of $N_0(t_2-t_1)(g-h)$ layers are completed. The layers completed at $t=t_1$ has length $2ht_1$; the layer completed at $t=t_2$ has length $2ht_2$. This information uniquely determines the angle θ in terms of b, N_0, g and h

for P an induction term that becomes negligible at large t. An equal number of steps have 'escaped' from the left side of the system. Equation (8) actually represents, of course, the number of layers completed up to time t. In the time interval (t_1, t_2) a total number of layers equal to $N_0(t_2-t_1)$ $(g-h)$ having total thickness $bN_0(t_2-t_1)$ $(g-h)$ are laid down. The first layer has length $2ht_1$, the last $2ht_2$. As indicated in *Figure 3*, this implies that:

$$\tan\theta=\frac{h}{bN_0(g-h)} \tag{9}$$

where θ (defined in *Figure 3*) characterizes the shape of the growing sector. Complete determination of θ must await a determination of N_0.

We now consider solutions in the interval $|x|<ht$. On the basis of the above-mentioned computer simulations, we expect that the steady-state solutions are functions of the quantity $u=x/t$ only. The ultimate justification of this statement is that this assumption leads to the correct solution. We also split r and l into odd and even parts. Therefore we assume:

$$r=\phi_1(u)+\phi_2(u) \tag{10}$$

where ϕ_1 is even in x (and u) and ϕ_2 is odd in x (and u), for $u=x/t$. Equation (5) then implies that:

$$l=\phi_1(u)-\phi_2(u) \tag{11}$$

Inserting these in the differential equations and separating odd and even parts yields:

$$\frac{1}{t}\left(g\frac{\mathrm{d}\phi_1}{\mathrm{d}u}-u\frac{\mathrm{d}\phi_2}{\mathrm{d}u}\right)=0 \tag{12}$$

$$\frac{1}{t}\left(g\frac{\mathrm{d}\phi_2}{\mathrm{d}u}-u\frac{\mathrm{d}\phi_1}{\mathrm{d}u}\right)=-2g(\phi_1^2-\phi_2^2)+i \tag{13}$$

In the steady state (large t), the left-hand side of equation (13) can be set equal to zero. Therefore, the steady-state solution obeys:

$$g\frac{\mathrm{d}\phi_1}{\mathrm{d}u}=u\frac{\mathrm{d}\phi_2}{\mathrm{d}u} \tag{14}$$

and

$$\phi_1^2-\phi_2^2=\frac{i}{2g} \tag{15}$$

The following function satisfies equations (14) and (15):

$$\phi_1=\left(\frac{i}{2g}\right)^{1/2}\frac{g}{(g^2-u^2)^{1/2}} \tag{16}$$

From this we may immediately write:

$$r(x,t)=\left[\left(\frac{i}{2g}\right)\left(\frac{gt+x}{gt-x}\right)\right]^{1/2} \tag{17}$$

$$l(x,t)=\left[\left(\frac{i}{2g}\right)\left(\frac{gt-x}{gt+x}\right)\right]^{1/2} \tag{18}$$

We notice immediately that equations (17) and (18) fail to satisfy the boundary conditions (equations (4)). The reason for this becomes apparent from equation (13). We see that $\phi_1^2-\phi_2^2$ is just the product rl, which according to equation (4) becomes very small near the boundaries. Therefore, near the boundaries, the right-hand side of equation (13) is very nearly i, and it is not appropriate to set the left-hand side of equation (13) equal to zero. Therefore, equations (17) and (18) are valid everywhere except near the boundaries. It also follows that the assumption of dependence on $u=x/t$ fails near the boundaries. The afore-mentioned computer simulations failed to detect this fact because of sampling errors.

Therefore, we expect correction terms that are significant near the boundaries. In the steady state, we expect these to be functions only of the distance from the boundary, and to be significant only over distances much smaller than ht. Therefore, we write:

$$r(x,t)=\left[\left(\frac{i}{2g}\right)\left(\frac{gt+x}{gt-x}\right)\right]^{1/2}+f_1(x+ht)+f_2(ht-x) \tag{19}$$

where f_1 and f_2 are functions to be determined. We assume that both f_1 and f_2 are non-negligible only for small values of their arguments, decaying to zero over distances much smaller than ht. Therefore, in equation (19), $f_1(x+ht)$ is significant only near $x=-ht$, and $f_2(x-ht)$ at $x=+ht$. Equation (5) demands:

$$l(x,t)=\left[\left(\frac{i}{2g}\right)\left(\frac{gt-x}{gt+x}\right)\right]^{1/2}+f_1(ht-x)+f_2(ht+x) \tag{20}$$

In equation (20), f_1 is significant only near $x=ht$, f_2 near $x=-ht$. Now write:

$$y_1=ht+x \qquad y_2=ht-x \tag{21}$$

Then

$$r(x,t)=\left[\left(\frac{i}{2g}\right)\left(\frac{gt+x}{gt-x}\right)\right]^{1/2}+f_1(y_1)+f_2(y_2) \tag{22}$$

$$l(x,t)=\left[\left(\frac{i}{2g}\right)\left(\frac{gt-x}{gt+x}\right)\right]^{1/2}+f_1(y_2)+f_2(y_1) \tag{23}$$

These have for derivatives:

$$\frac{\partial r}{\partial x}=\left(\frac{i}{2g}\right)^{1/2}gt(gt+x)^{-1/2}(gt-x)^{-3/2}+f'_1(y_1)-f'_2(y_2) \tag{24}$$

$$\frac{\partial r}{\partial t}=-\left(\frac{i}{2g}\right)^{1/2}gx(gt+x)^{-1/2}(gt-x)^{-3/2}+hf'_1(y_1)+hf'_2(y_2) \tag{25}$$

where f'_1 and f'_2 are the derivatives of f_1 and f_2 respectively. Inserting equations (22)–(25) into equation (2a) yields:

$$\left(\frac{i}{2g}\right)^{1/2} g(gt+x)^{-1/2}(gt-x)^{-1/2} + (h+g)f'_1(y_1)+(h-g)f'_2(y_2)$$
$$= -2g\left[\left(\frac{i}{2g}\right)^{1/2}\left(\frac{gt+x}{gt-x}\right)^{1/2}[f_1(y_2)+f_2(y_1)] + \left(\frac{i}{2g}\right)^{1/2}\left(\frac{gt-x}{gt+x}\right)^{1/2}[f_1(y_1)+f_2(y_2)] + [f_1(y_1)+f_2(y_2)][f_2(y_1)+f_1(y_2)]\right] \quad (26)$$

The first term on the left-hand side of equation (26) is $O(1/t)$ and we therefore drop it. Let us proceed by replacing x everywhere in equation (26) with y_1-ht and assume that y_1 is small. Then y_2 is near $2ht$ and $f_1(y_2)$, $f_2(y_2)$, $f'_1(y_2)$ and $f'_2(y_2)$ are all negligible. We obtain:

$$(h+g)f'_1(y_1) = -2g\left[\left(\frac{i}{2g}\right)^{1/2}\left(\frac{g-h}{g+h}\right)^{1/2} f_2(y_1) + \left(\frac{i}{2g}\right)^{1/2}\left(\frac{g+h}{g-h}\right)^{1/2} f_1(y_1) + f_1(y_1)f_2(y_1)\right] \quad (27)$$

Likewise, we may set $x=ht-y_2$ and assume that y_2 is small. We obtain:

$$(h-g)f'_2(y_2) = -2g\left[\left(\frac{i}{2g}\right)^{1/2}\left(\frac{g+h}{g-h}\right)^{1/2} f_1(y_2) + \left(\frac{i}{2g}\right)^{1/2}\left(\frac{g-h}{g+h}\right)^{1/2} f_2(y_2) + f_2(y_2)f_1(y_2)\right] \quad (28)$$

The right-hand side of equation (28) becomes identical to the right-hand side of equation (27) if we replace y_2 with y_1. Therefore:

$$(h-g)\,\mathrm{d}f_2 = (h+g)\,\mathrm{d}f_1 \quad (29)$$

which implies:

$$f_2 = \left(\frac{h+g}{h-g}\right) f_1 \quad (30)$$

No constant of integration appears in equation (30) since we know both functions decay to zero. Inserting equation (30) into equation (27) and rearranging yields:

$$\frac{\mathrm{d}f_1}{\mathrm{d}y} = \frac{2g}{g-h} f_1^2 \quad (31)$$

which implies:

$$[f_1(y)]^{-1} = \frac{-2gy}{g-h} + C \quad (32)$$

The constant of integration, C, is chosen to satisfy equation (4a):

$$0 = r(-ht) = \left(\frac{i}{2g}\right)^{1/2}\left(\frac{g-h}{g+h}\right)^{1/2} + f_1(0) + f_2(2ht) \quad (33)$$

implying:

$$C = -\left(\frac{2g}{i}\right)^{1/2}\left(\frac{g+h}{g-h}\right)^{1/2} \quad (34)$$

Our final result is:

$$r(x,t) = \left[\left(\frac{i}{2g}\right)\left(\frac{gt+x}{gt-x}\right)\right]^{1/2} - \frac{1}{\beta_1+\alpha_1 x} + \frac{1}{\beta_2+\alpha_2 x} \quad (35)$$

with

$$\alpha_1 = 2g/(g-h) \quad (36)$$

$$\beta_1 = \frac{2ght}{g-h} + \left(\frac{2g}{i}\right)^{1/2}\left(\frac{g+h}{g-h}\right)^{1/2} \quad (37)$$

$$\alpha_2 = -2g/(g+h) \quad (38)$$

$$\beta_2 = \frac{2ght}{g+h} + \left(\frac{2g}{i}\right)^{1/2}\left(\frac{g-h}{g+h}\right)^{1/2} \quad (39)$$

Setting $x=ht$ in equation (35) yields the following expression for N_0:

$$N_0 = 2\left(\frac{i}{2g}\right)^{1/2}\left(\frac{g+h}{g-h}\right)^{1/2} \quad (40)$$

Inserting this into equation (9) yields:

$$\tan\theta = \frac{h}{b}\left(\frac{g}{2i(g^2-h^2)}\right)^{1/2} \quad (41)$$

We now compute the shape of the growth front. The growth-front profile is given by the following expression:

$$\Gamma(x,t) = b\int_{-ht}^{x} [l(x',t)-r(x',t)]\,\mathrm{d}x' \quad (42)$$

$\Gamma(x,t)$ is defined by counting all the steps between $-ht$ and x at a given time, and adding $+b$ for each left-moving step and $-b$ for each right-moving step. The integrand in equation (42) may be written in this way:

$$l-r = \left(\frac{i}{2g}\right)^{1/2}\left(\frac{-2x}{(g^2t^2-x^2)^{1/2}}\right) - \frac{2\alpha_1 x}{\beta_1^2-\alpha_1^2x^2} + \frac{2\alpha_2 x}{\beta_2^2-\alpha_2^2x^2} \quad (43)$$

Upon integration, the last two terms contribute only $\ln(t)$ terms, while the first contributes a term linear in t. Therefore, at long times, we only need consider the first term of equation (43). The result is:

$$\Gamma(x,t) = 2b(i/2g)^{1/2}t\{[g^2-(x/t)^2]^{1/2} - [g^2-h^2]^{1/2}\} \quad (44)$$

Equation (44) is a section of an ellipse. *Figure 4* displays a graph of $\Gamma(x,t)$ for certain values of g and h. Note that $\Gamma(\pm ht,t)$ is zero, while

$$\Gamma(0,t) = bt(2ig)^{1/2}\{1-[1-(h/g)^2]^{1/2}\} \quad (45)$$

In the limit $g \gg h$, the growth profile is observed to be flat.

SHAPE OF A HYPOTHETICAL CRYSTAL

As an illustrative example, we examine the shape of a hypothetical crystal, formed of six sectors as shown in *Figure 5*. The structure is intended to be suggestive of polyethylene single crystals, although a more complete treatment of polyethylene crystals appears elsewhere[6]. The crystal is formed of four sectors that grow with flat edges and at a velocity vector G_1 inclined at an angle λ relative to the horizontal, and of two sectors that grow according to the equations given in the last section, with

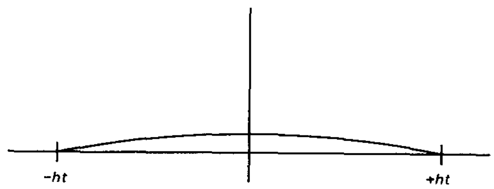

Figure 4 Function $\Gamma(x,t)$ computed for particular values of g and h

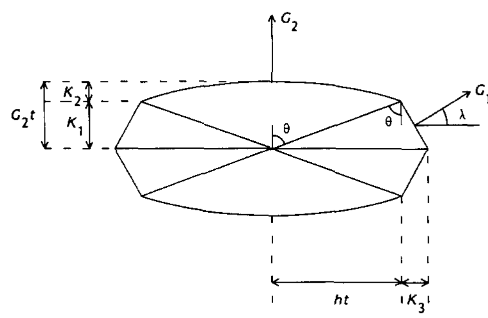

Figure 5 Shape of a hypothetical crystal as predicted by the present analysis

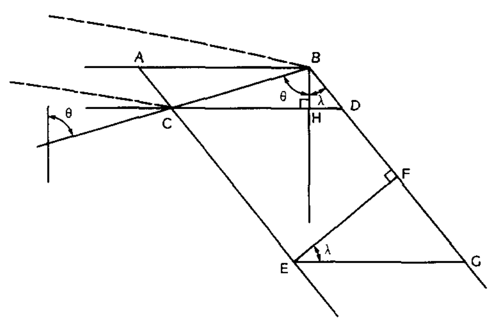

Figure 6 Diagram illustrating the derivation of equation (47)

velocity G_2 directed vertically. To save space, we introduce the trigonometric substitution:

$$\cos\phi = h/g \tag{46}$$

valid whenever $h<g$. Then the expression $[1-(h/g)^2]^{1/2}$ which appears frequently may be written $\sin\phi$. *Figure 6* is a blown-up view of the region near the intersection of the growth fronts of the two sectors, showing the change in the crystal during a time interval Δt. During the time interval, the edge of the flat sector moves from the line CE to the line BG. The broken curves passing through C and B respectively represent the growth front of the curved sector before and after the time interval Δt. Let d(AB) represent the distance between the two points A and B, and let a(ABC) represent the value of the angle formed by the three points A, B and C. Then from *Figure 6* it is obvious that: $d(\mathrm{EF})=G_1\Delta t$, $d(\mathrm{EG})=d(\mathrm{CD})=(G_1/\cos\lambda)\Delta t$, $a(\mathrm{HBD})=\lambda$, $d(\mathrm{CH})=h\Delta t$, $d(\mathrm{BH})=h\Delta t/\tan\theta$, $\tan\lambda=d(\mathrm{HD})/d(\mathrm{BH})$ and $d(\mathrm{HD})=h\Delta t(\tan\lambda/\tan\theta)$. Therefore, requiring $d(\mathrm{CH})=d(\mathrm{CD})-d(\mathrm{HD})$ implies:

$$h=\frac{G_1}{\cos\lambda}-\frac{h\tan\lambda}{\tan\theta} \tag{47}$$

from which we may write:

$$h=\frac{G_1\tan\theta}{\cos\lambda\,(\tan\theta+\tan\lambda)} \tag{48}$$

The distance K_1 in *Figure 5* is given by:

$$K_1=\frac{ht}{\tan\theta}=tb(2ig)^{1/2}\sin\phi \tag{49}$$

The distance K_2, given by equation (45), is:

$$K_2=tb(2ig)^{1/2}(1-\sin\phi) \tag{50}$$

When we require $G_2t=K_1+K_2$, we obtain:

$$G_2=b(2ig)^{1/2} \tag{51}$$

which is the expected result for regime II crystallization[4]. By combining equations (41) and (51), we obtain the following for $\tan\theta$:

$$\tan\theta=\frac{h}{G_2\sin\phi} \tag{52}$$

Then by combining equations (47) and (52), we obtain:

$$h=G_1/\cos\lambda-G_2\tan\lambda\sin\phi \tag{53}$$

The distance K_3 in *Figure 5* is $ht(\tan\lambda/\tan\theta)$. If we define the aspect ratio of the crystal as the ratio of $ht+K_3$ to G_2t we obtain:

$$A=\frac{h}{G_2}\left(1+\frac{\tan\lambda}{\tan\theta}\right) \tag{54}$$

Inserting the expression for h given by equation (48) into equation (54) yields:

$$A=\frac{G_1}{G_2\cos\lambda} \tag{55}$$

as expected. The curvature of the curved sectors, defined as the ratio of K_2 to $2ht$, is:

$$C=\frac{G_2}{2h}(1-\sin\phi) \tag{56}$$

The following expression, which can be determined geometrically or verified by direct substitution, also holds:

$$A=\frac{\tan\theta+\tan\lambda}{1+2C\tan\theta} \tag{57}$$

If one regards A, C and λ as given, then equation (57) permits determination of $\tan\theta$. Then equation (55) yields the ratio G_2/G_1; equation (54) yields h/G_1; equation (52) yields $\sin\phi$ and therefore g/G_1. On the other hand, if we regard λ, g/G_1, and G_2/G_1 as given, then we must solve parametrically an equation such as equation (53) for h/G_1, since ϕ depends on h. After this, all the other parameters may be calculated. For example, the structure shown in *Figure 5* is completely determined by specifying $A=2.408$, $C=0.0732$ and $\lambda=\pi/6$; or equivalently, by specifying $g/G_1=1.356$, $G_2/G_1=0.4795$ and $\lambda=\pi/6$.

DISCUSSION

The crystal shape shown in *Figure 5* is suggestive of the polyethylene single crystals that grow with curved growth fronts under certain conditions[7]. However, to obtain appreciable curvature using the present model, we must select g near h (see equations (45) or (50)). This creates a problem, because on the basis of standard nucleation theory, one expects $h\ll g$, which leads to flat growth profiles, by equation (45). Indeed, the experimentally observed curved crystals have led some workers to challenge the validity of the standard nucleation model[8].

However, it is shown elsewhere that these crystals are expected to be strained[6], and that this strain can produce values of g near h.

Although we have not considered the case of $h > g$, we can make some statements about the solutions one would expect to find. Note first of all that a layer is only completed when steps meet the boundaries at $\pm ht$. If h is greater than g, no steps can ever reach the boundaries, and no layer is ever completed. As the boundaries move apart, nucleation on virgin substrate would continually create patches that spread to join the first layer, and likewise for all succeeding layers. Therefore, one would expect all layers to continue to grow and that θ would always equal 90°. Therefore, the case of $h > g$ cannot apply to the growth of sectored crystals, and we are justified in neglecting it here.

ACKNOWLEDGEMENTS

The author is grateful to Dr J. D. Hoffman and Dr R. L. Miller, both of the Michigan Molecular Institute, for a number of helpful discussions. Special thanks also go to Dr F. Khoury of the National Bureau of Standards for bringing a mistake in the original manuscript to the attention of the author. Partial support for this research has been provided by the National Science Foundation, Grant No. DMR-8607708.

REFERENCES

1 Hoffman, J. D., Davis, G. T. and Lauritzen, J. I., Jr. in *Treatise on Solid State Chemistry* (Ed. N. B. Hannay), Plenum Press, New York, 1976, Vol. 3
2 Hoffman, J. D. *Polymer* 1985, **26**, 1763
3 Sanchez, I. C. and DiMarzio, E. A. *J. Res. Nat. Bur. Stand.* 1972, **76A**, 213; Lauritzen, J. I., Jr. *J. Appl. Phys.* 1973, **44**, 4353; Hoffman, J. D., Ross, G. S., Frolen, L. and Lauritzen, J. I., Jr. *J. Res. Nat. Bur. Stand.* 1975, **79A**, 671; Hoffman, J. D. *Polymer* 1983, **24**, 3; Guttman, C. M. and DiMarzio, E. A. *J. Appl. Phys.* 1983, **54**, 5541
4 Frank, F. C. *J. Cryst. Growth* 1974, **22**, 233
5 Toda, A., Kiho, H., Miyaji, H. and Asai, K. *J. Phys. Soc. Japan* 1985, **54**, 1411; Toda, A. and Tanzawa, Y. *J. Cryst. Growth* 1986, **76**, 462; Toda, A. *J. Phys. Soc. Japan* 1986, **55**, 3419
6 Mansfield, M. L. manuscript in preparation; Hoffman, J. D. manuscript in preparation
7 Organ, S. J. and Keller, A. *J. Mater. Sci.* 1985, **20**, 1571, 1586, 1602; Organ, S. J. and Keller, A. *J. Polym. Sci., Polym. Phys. Edn.* 1986, **24**, 2319
8 Sadler, D. M. and Gilmer, G. H. *Polymer* 1984, **25**, 1446; Sadler, D. M. *Polym. Commun.* 1986, **27**, 149; Sadler, D. M. *J. Polym. Sci., Polym. Phys. Edn.* 1985, **23**, 1533; Sadler, D. M. and Gilmer, G. H. *Phys. Rev. Lett.* 1986, **56**, 2708; Sadler, D. M. *Polymer* 1987, **28**, 1440

Note added in proof

Reference 9 also considers the problem of crystal growth habit, and therefore is relevant to the third section of this paper.

9 Passaglia, E. and Khoury, F. *Polymer* 1984, **25**, 631; Passaglia, E. and Di Marzio, E. A. *Polymer* 1986, **27**, 510